European Journal of Medicinal Chemistry 69 (2013) 216–222

Contents lists available at ScienceDirect

European Journal of Medicinal Chemistry

journal homepage: http://www.elsevier.com/locate/ejmech

Original article

Biological activity of neutral and cationic iridium(III) complexes with κ*P* and κ*P*,κ*S* coordinated $Ph_2PCH_2S(O)_xPh$ ($x = 0–2$) ligands

Gerd Ludwig [a], Sanja Mijatović [b], Ivan Ranđelović [b], Mirna Bulatović [b], Djordje Miljković [b], Danijela Maksimović-Ivanić [b], Marcus Korb [c], Heinrich Lang [c], Dirk Steinborn [a], Goran N. Kaluđerović [a,*]

[a] Institute of Chemistry, Martin Luther University Halle-Wittenberg, Kurt-Mothes-Straße 2, D-06120 Halle, Germany
[b] Institute for Biological Research "Sinisa Stankovic", University of Belgrade, Bulevar despota Stefana 142, 11060 Belgrade, Serbia
[c] Institute of Chemistry, Chemnitz University of Technology, Straße der Nationen 62, D-09111 Chemnitz, Germany

ARTICLE INFO

Article history:
Received 8 May 2013
Received in revised form
12 August 2013
Accepted 14 August 2013
Available online 29 August 2013

Keywords:
Iridium(III) complexes
Sulfur-functionalized phosphorus ligands
Cytotoxic activity

ABSTRACT

Neutral iridium(III) complexes of the type $[Ir(\eta^5\text{-}C_5Me_5)Cl_2\{Ph_2PCH_2S(O)_xPh\text{-}\kappa P\}]$ (**1**–**3**) with diphenylphosphino-functionalized methyl phenyl sulfides, sulfoxides, and sulfones $Ph_2PCH_2S(O)_xPh$ ($x = 0$, **L1**; 1, **L2**; 2, **L3**) and the cationic complex $[Ir(\eta^5\text{-}C_5Me_5)Cl\{Ph_2PCH_2SPh\text{-}\kappa P,\kappa S\}][PF_6]$ (**4**) were synthesized and fully characterized analytically and spectroscopically. Furthermore, the structure of **2** was determined by X-ray diffraction analysis. The biological potential of the neutral and cationic iridium(III) complexes was tested *in vitro* against the cell lines 8505C, A253, MCF-7, SW480 and 518A2. Complex $[Ir(\eta^5\text{-}C_5Me_5)Cl_2\{Ph_2PCH_2S(O)Ph\text{-}\kappa P\}]$ (**2**), with ligand **L2** κ*P* coordinated containing a pendent sulfinyl group, is the most active one (IC_{50} values of about 3 μM), thus, with activities comparable to cisplatin. Complex **2** proved to have an even a higher antiproliferative activity than cisplatin against 8505C and SW480 cell lines, used as a model system of highly anaplastic cancers with low sensitivity to conventional chemotherapeutics such as cisplatin. Additional experiments demonstrated that apoptosis and autophagic cell death contribute to the drug's tumoricidal action.

1. Introduction

Bioinorganic chemistry is a fast-growing area of fascinating opportunities and creative power [1]. This is reflected, among others, in the discovery of the cancerostatic activity of cisplatin by Rosenberg in 1965 [2,3]. Cisplatin itself is still used and is considered a benchmark for the entire field of metal-based anticancer drugs that have since been developed [4]. Due to the disadvantage of the dose-dependent side effects of cisplatin as well as the resistance of some carcinomas, it is understandable that a wide range of novel transition metal complexes were screened for their use as therapeutic agents [5–10]. Thus, first promising steps were taken in the field of titanium-, ruthenium- and gold-based anticancer agents [11]. For instance, the octahedral ruthenium(III) complexes [imiH]*trans*-[Ru(imi-κ*N*)(dmso-κ*S*)Cl_4] (imi = imidazole) and [indH]*trans*-[Ru(ind-κ*N*)$_2Cl_4$] (ind = indazole) have reached clinical trials for cancer treatment [12–17]. On the other hand, only a few steps have been taken in the field of iridium-based anticancer agents [18–25]. This can be, at least in part, attributed to the relatively high kinetic inertness of iridium(III) complexes due to their low-spin d^6 valence electron configuration [26]. On this basis, for example, the absence of cytotoxic activity of the iridium(III) complexes [imiH]*trans*-[Ir(imi-κ*N*)(dmso-κ*S*)Cl_4] and [indH]*trans*-[Ir(ind-κ*N*)$_2Cl_4$] has been explained [27]. Despite these initial setbacks, iridium(III) complexes such as *fac*-[Ir(N^N)(dmso-κ*S*)Cl_3] (N^N = diimine type ligand) **I** (Fig. 1) [28], with a promising anticancer activity have been prepared. On a broad scale η^5-pentamethylcyclopentadienyl iridium(III) complexes of the type $[Ir(\eta^5\text{-}C_5Me_5)Cl(X^{\cap}Y)]^{n+}$ (X^Y = bidentate ligand) have been tested for their ability to decrease the cell viability. Originally, compounds with *N*,*N*' ligands (X^Y = ethylendiamine, 2,2′-bipyridine, 1,10-phenanthroline) [29] as well as $[Ir(\eta^5\text{-}C_5Me_5)Cl_2(PTA)]$ (PTA = 1,3,5-triaza-7-phosphaadamantane) [23] were found to have no cytotoxicity against several cancer cell lines. On the other hand, Sheldrick et al. [30] and Sadler et al. [29] found that complexes of the above mentioned type bearing a functionalized bipyridine or phenanthroline ligand and a functionalized C_5Me_5 ligand, respectively, as shown in the examples **II** and **III** (Fig. 1), exhibited high

* Corresponding author. Tel.: +49 345 5525678; fax: +49 345 5527028.
E-mail address: goran.kaluderovic@chemie.uni-halle.de (G.N. Kaluđerović).

0223-5234/$ – see front matter © 2013 Elsevier Masson SAS. All rights reserved.
http://dx.doi.org/10.1016/j.ejmech.2013.08.025

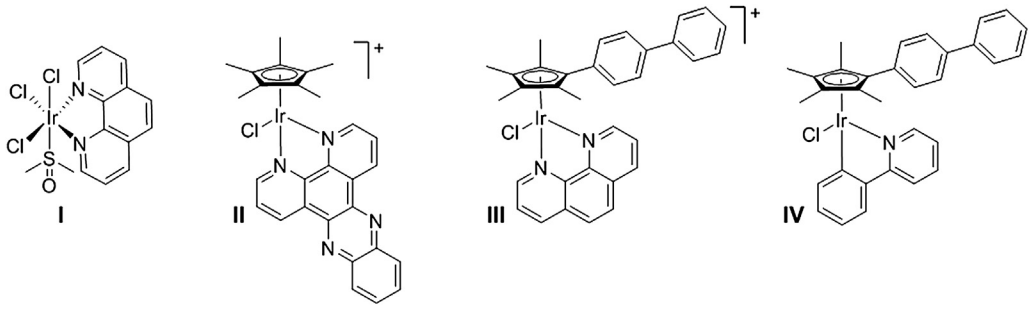

Fig. 1. Examples of iridium-based anticancer drugs.

biological potential. Furthermore, complex **IV** (Fig. 1) bearing an anionic N^C ligand, instead of a neutral diimine type ligand (such as bpy), possess a promising anticancer ability with IC_{50} value (IC_{50} = concentration of compound that inhibits 50% of cell growth) of 0.7 μM (cell line A2780), which is comparable to that of cisplatin (IC_{50} = 1.2 μM) [31,32].

To the best of our knowledge, no cytotoxically active iridium(III) complexes with phosphorus ligands have been reported so far. Previously, our group has reported on neutral and cationic ruthenium(II) complexes with ω-diphenylphosphino-functionalized alkyl phenyl sulfides, sulfoxides and sulfones that exhibit promising anticancer activity, partially by one order of magnitude higher in activity than cisplatin [33,34]. Here, we report on the biological potential of iridium(III) complexes of the type [Ir(η^5-C_5Me_5)Cl_2{$Ph_2PCH_2S(O)_x$Ph-κ*P*}] and [Ir(η^5-C_5Me_5)Cl{Ph_2PCH_2SPh-κ*P*,κ*S*}][PF_6], especially on a correlation between the oxidation state of the sulfur atom (x = 0–2) and the cytotoxic activity as well as on the tumoricidal action of these anticancer drugs.

2. Results and discussion

2.1. Syntheses and characterization

Mononuclear neutral iridium(III) complexes of the type [Ir(η^5-C_5Me_5)Cl_2{$Ph_2PCH_2S(O)_x$Ph-κ*P*}] (**1**–**3**) were synthesized through reactions of the dinuclear complex [{Ir(η^5-C_5Me_5)Cl_2)}$_2$] with diphenylphosphino-functionalized methyl phenyl sulfides, sulfoxides, and sulfones $Ph_2PCH_2S(O)_xPh$ (x = 0, **L1**; 1, **L2**; 2, **L3**) in methylene chloride (Scheme 1, reaction pathway **a**). As reported for complex **1** [35] and also for other cases [36], the donicity of the P atom is high enough to cleave the Ir–Cl–Ir bridges. Furthermore, the cationic iridium(III) complex [Ir(η^5-C_5Me_5)Cl{Ph_2PCH_2SPh-κ*P*,κ*S*}][PF_6] (**4**) was obtained through chlorido abstraction with [NH_4][PF_6] starting from the corresponding neutral iridium(III) complex **1** (Scheme 1, reaction pathway **b**). The complexes **1**–**3** were obtained as orange powders in yields between 64 and 71% and the cationic complex **4** as reddish powder in a yield of 77%. Both, the neutral and the cationic complexes **1**–**4** are stable in air over weeks and soluble in methylene chloride and dimethyl sulfoxide. The identities of complexes **1**–**4** were confirmed by elemental analyses, NMR spectroscopy (^{1}H, ^{13}C, ^{31}P), and X-ray single-crystal structure analysis (**2**).

All ^{1}H, ^{13}C, and ^{31}P NMR spectroscopic parameters of complexes **1**–**4** are in the expected range; selected values are given in Table 1 [35]. Coordination-induced shifts (CIS) of the α-carbon atoms ($\delta_{C(coord.)} - \delta_{C(uncoord.)}$) of the ligands $Ph_2PCH_2S(O)_xPh$ were found between −2.9 and −3.6 ppm. Furthermore, κ*P* coordination of the ligands to Ir(III) results in CIS of the phosphorus resonances ($\delta_{P(coord.)} - \delta_{P(uncoord.)}$) between 20 and 24 ppm. In contrast, the additional *S* coordination of **L1** in complex **4** results in a high-field shift of the phosphorus resonance by −14 ppm. Whereas in the uncoordinated ligands the magnitude of the $^1J_{P,C}$ coupling constants of the α-carbon atoms are in direct relation to the oxidation state of the sulfur atom ($^1J_{P,C}$ = 23.2 Hz (**L1**) < 31.2 Hz (**L2**) < 35.7 Hz (**L3**)), the coordination to Ir(III) aligns all the $^1J_{P,C}$ coupling constants at about 26 Hz. The resonances of the η^5-C_5Me_5 ligand in complexes **1**–**3** are in a narrow range and, thus, they are not dependent on the pendent $S(O)_xPh$ group. Even the values of the cationic complex **4** differ only marginally (Table 1).

Crystals of [Ir(η^5-C_5Me_5)Cl_2{$Ph_2PCH_2S(O)Ph$-κ*P*}] (**2**) suitable for X-ray diffraction analysis were obtained from solutions of methylene chloride/*n*-pentane at room temperature. The compound crystallized as isolated molecules without unusual intermolecular interactions (shortest distance between non-hydrogen atoms: 3.370(3) Å, C12···C28′). The molecular structure is shown in Fig. 2 and selected structural parameters are given in the figure caption.

The iridium(III) complex adopts a typical half sandwich ("three-legged piano stool") structure, in which the metal center is coordinated to a η^5-C_5Me_5 ligand (distance Ir to ring centroid 1.835 Å), two chlorido ligands as well as the $Ph_2PCH_2S(O)Ph$-κ*P* (**L2**) ligand. The angles at the iridium(III) atom are close to 90° (86.7(1)–89.8(2)°), so that the structure can be viewed as a distorted octahedron. The Ir–Cl bond lengths (2.407(3)/2.401(3) Å) as also the Ir–P bond length (2.310(3) Å) are in the expected range (median Ir–Cl: 2.419 Å, lower/higher quartile: 2.315/2.606 Å, n = 543; median Ir–P: 2.316 Å, lower/higher quartile: 2.151/2.462 Å, n = 543; n – number of observations [37]).

2.2. Biological studies

To evaluate the cytotoxic potency of the iridium(III) complexes **1**–**4**, 8505C human thyroid carcinoma, A253 submandibular carcinoma, MCF-7 breast adenocarcinoma, SW480 colon adenocarcinoma, and 518A2 melanoma cell lines were exposed to a wide range of doses of these compounds. Cell viability was estimated after 96 h by SRB assay [38]. According to the obtained results all complexes expressed a dose-dependent decrease of cell viability (Fig. 3). The IC_{50} values of iridium(III) complexes **1**–**4** are listed in Table 2; the activities of cisplatin are included for comparison. For further understanding the IC_{50} values of the corresponding ligands **L1**–**L3** and the related ruthenium complexes are given in Table S1.

Generally, the phosphine–sulfide **L1** and the phosphine–sulfoxide **L2** possess an up to forty times lower *in vitro* activity than the related iridium(III) complexes. The activities of the phosphine–sulfone **L3** are similar and in two cases (cell lines 518A2 and 8505C) even three times better than those of the corresponding iridium(III) complex **3**. The only complex with activities comparable to cisplatin is [Ir(η^5-C_5Me_5)Cl_2{$Ph_2PCH_2S(O)Ph$-κ*P*}] (**2**) with ligand **L2** κ*P* coordinated containing a pendent sulfinyl group (IC_{50} values of about 3 μM). Thus, **2** exhibited slightly higher antiproliferative activity

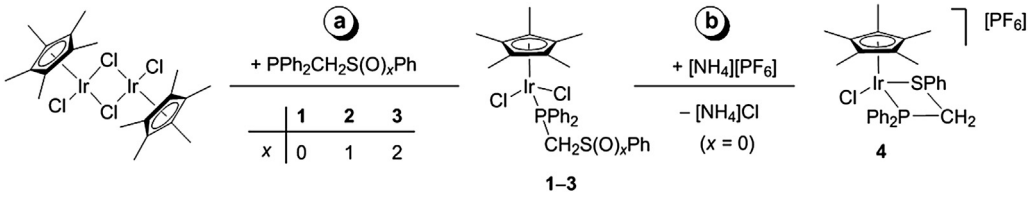

Scheme 1. Synthetic routes to iridium(III) complexes bearing $Ph_2PCH_2S(O)_xPh$-κ*P* ligands (**1**–**3**) and the Ph_2PCH_2SPh-κ*P*,κ*S* ligand (**4**), respectively.

than cisplatin on the cisplatin resistant cell lines 8505C and SW480, whereas on two cisplatin sensitive cell lines (518A2 and A253) **2** was found twice less efficient than cisplatin. It is worth mentioning that the iridium(III) complex **2** exhibited higher activities (up to one order of magnitude) on all tested cell lines than the related ruthenium(II) complex $[Ru(\eta^6\text{-}p\text{-cym})Cl_2\{Ph_2PCH_2S(O)Ph\text{-}\kappa P\}]$ [33]. This result is in contrast to the iridium(III) complexes **1**, **3**, and **4** with the sulfide- (**L1**) and sulfonyl-functionalized ligand (**L3**), that exhibited a comparable or even less ability to decrease the cell viability in comparison with the analogous ruthenium(II) complexes $[Ru(\eta^6\text{-}p\text{-cym})Cl_2\{Ph_2PCH_2S(O)_xPh\text{-}\kappa P\}]/[Ru(\eta^6\text{-}p\text{-cym})Cl\{Ph_2PCH_2SPh\text{-}\kappa P,\kappa S\}][PF_6]$ ($x = 0, 2$) [33,34]. The neutral complex $[Ir(\eta^5\text{-}C_5Me_5)Cl_2\{Ph_2PCH_2SPh\text{-}\kappa P\}]$ (**1**) and the corresponding cationic complex $[Ir(\eta^5\text{-}C_5Me_5)Cl\{Ph_2PCH_2SPh\text{-}\kappa P,\kappa S\}][PF_6]$ (**4**), containing the Ph_2PCH_2SPh ligand κ*P* and κ*P*,κ*S* coordinated, respectively, exhibited similar antitumor activities against investigated cell lines, with the exception of the 518A2 cell line. These findings are in contrast to the analogous ruthenium(II) complexes $[Ru(\eta^6\text{-}p\text{-cym})Cl\{Ph_2PCH_2SPh\text{-}\kappa P,\kappa S\}][PF_6]$ and $[Ru(\eta^6\text{-}p\text{-cym})Cl_2\{Ph_2PCH_2SPh\text{-}\kappa P\}]$, where the cationic complex exhibited an up to sixteen times higher inhibition than the neutral one against three cell lines (8505C, MCF-7, SW80) [34].

The sensitivity of the cancer cells under investigation (although derived from different origins and types of tumors) on $[Ir(\eta^5\text{-}C_5Me_5)Cl_2\{Ph_2PCH_2S(O)Ph\text{-}\kappa P\}]$ (**2**), the most potent complex, was similar. Because of low level of differentiation and dominant stem phenotype, 8505C thyroid carcinoma was selected for further analysis as a model of highly malignant and almost incurable type of the tumor. Thus, to explore the mechanism of action, 8505C cells were treated with the IC_{50} dose of complex **2** for 48 h. Then, the presence of early and late apoptotic cells were analyzed with double Ann/PI staining. As seen in Fig. 4A, in comparison to the control (non-treated cells), a 48 h treatment with **2** gave rise to an increase of both early apoptotic cells marked by externalization of phosphatidylserin and late apoptotic/necrotic cells stained by both Ann and PI. In parallel, 22% of cells displayed enhanced activation of caspases confirming that caspase-dependent apoptosis is probably behind the action of this compound (Fig. 4B). Accordingly, cell cycle analysis showed an increased percentage of hipodiploid cells with fragmented DNA upon treatment with **2** pointing out once more that apoptosis is the dominant mode of action of this kind of iridium-based drugs (Fig. 4C). In parallel, in the cytoplasm of cells exposed to **2** massive autophagic vesicles were determined indicating an enhanced autophagic process (Fig. 4D). Keeping in mind that autophagy serves to save the cells from damage, but can mediate cell death in some circumstances, cells were exposed to specific autophagic inhibitor 3-MA concomitantly with **2**. The measurement of the cell viability revealed a 10% increase in a number of tumor cells in cultures exposed to both **2** and the inhibitor in comparison to cultures exposed to the drug alone (Fig. 4E). This result confirms that besides apoptosis, autophagic cell death also contributes to the drugs tumoricidal action.

In an attempt to explore the involvement of oxidative stress in the cytotoxicity of **2**, cells were stained with the specific dye DHR (dihydrorhodamine 123) which became fluorescent in contact with reactive oxygen (ROS) and nitrogen species (RNS). The cumulative effect was measured after 24 and 48 h of exposure to **2**. Interestingly, instead of enhanced ROS and RNS levels, significantly decreased levels of free radicals were determined (Fig. 4F). The observed phenomenon was previously described in thyroid cancer

Table 1
Selected NMR spectroscopic data (δ in ppm, *J* in Hz) of $[Ir(\eta^5\text{-}C_5Me_5)Cl_2\{Ph_2PCH_2S(O)_xPh\text{-}\kappa P\}]$ (**1**–**3**) and $[Ir(\eta^5\text{-}C_5Me_5)Cl_2\{Ph_2PCH_2SPh\text{-}\kappa P,\kappa S\}][PF_6]$ (**4**).

	x[a]	$Ph_2PC_\alpha H_2S(O)_xPh$			C_5Me_5 (ring)		
		$\delta_{\alpha\text{-}CH}$ ($^1J_{P,H}$)	$\delta_{\alpha\text{-}C}$ ($^1J_{P,C}$)	δ_P	δ_H ($^4J_{P,H}$)	δ_{CMe} ($^3J_{P,C}$)	δ_C ($^2J_{P,C}$)
1	0 (κ*P*)	4.29 (4.8)	29.1 (26.8)	2.3	1.26 (2.3)	8.2 (1.0)	92.2 (2.8)
2	1 (κ*P*)	4.04–4.57	55.9 (25.4)	−4.8	1.37 (2.4)	8.0 (1.0)	92.5 (3.0)
3	2 (κ*P*)	3.96–4.01	56.5 (26.0)	−5.2	1.33 (2.4)	8.3	92.5
4	0 (κ*P*,κ*S*)	5.12–5.18	29.6	−31.9	1.73 (2.9)	8.7 (1.0)	92.3

[a] The coordination mode of the ligand is given in parentheses.

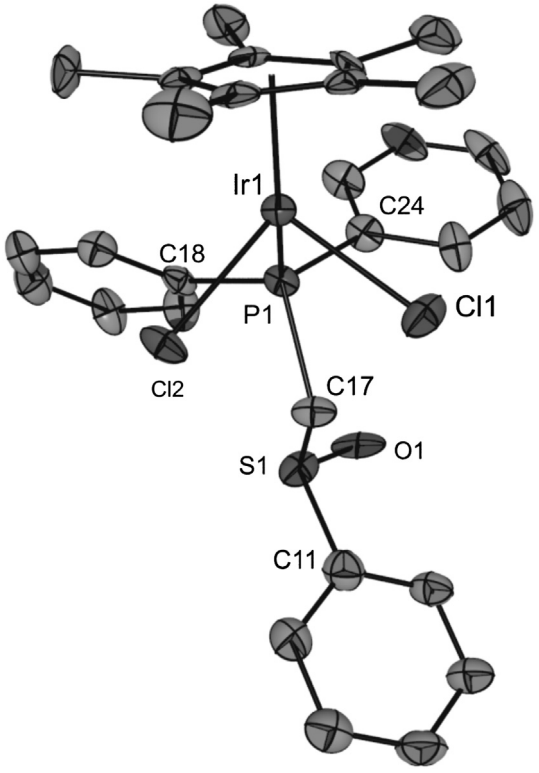

Fig. 2. Molecular structure of $[Ir(\eta^5\text{-}C_5Me_5)Cl_2\{Ph_2PCH_2S(O)Ph\text{-}\kappa P\}]$ in crystals of **2**. The ellipsoids are shown with a probability of 30%. From the disordered $PhS(O)CH_2$ group only the major occupied position is shown. H atoms have been omitted for clarity. Selected structural parameters (distances in Å, angles in °; values for the disordered group (63/37%) are given separated by a slash): Ir1–Cl1 2.407(3), Ir1–Cl2 2.401(3), Ir1–P1 2.310(3), Cl1–Ir1–Cl2 89.8(2), Cl1–Ir–P1 86.7(1), Cl2–Ir–P1 87.7(1), C11–S1–C17 93.3(1)/103(2), O1–S1–C17 115.5(2)/98(3), O1–S1–C11 102.7(1)/120(2).

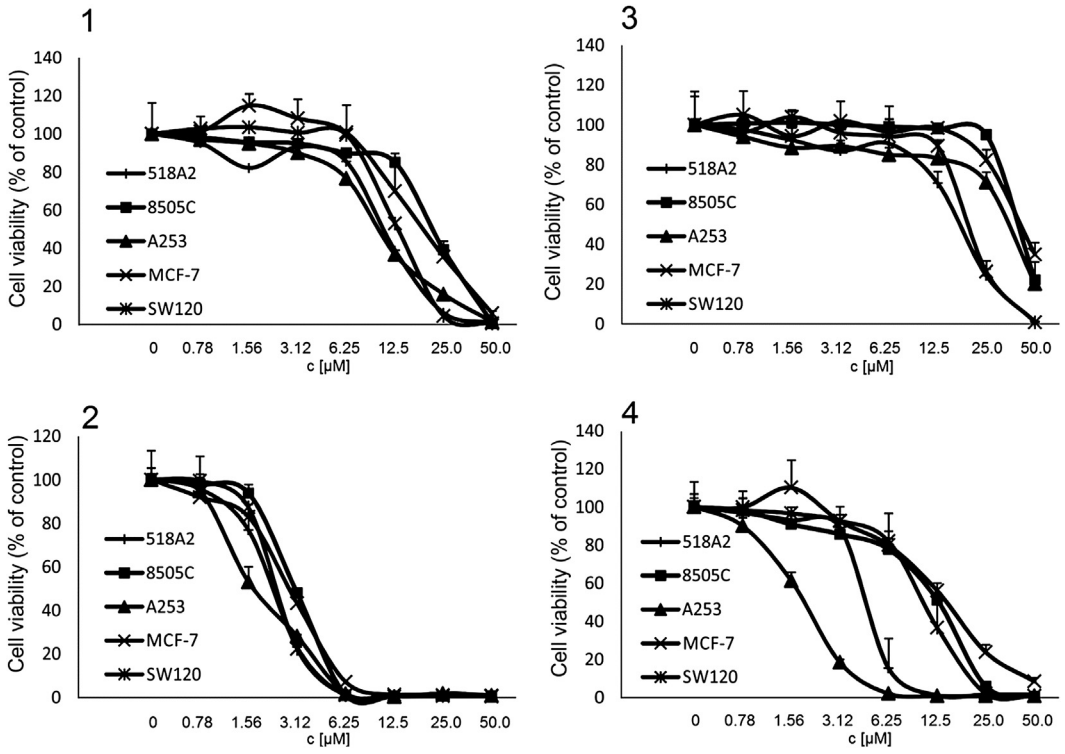

Fig. 3. Representative graphs showing survival (in %) of cells grown for 96 h in the presence of increasing concentrations of compounds **1**–**4**.

cells treated with proteasome inhibitor (bortezomib) and explained with cell-specific response to toxic stimuli [39,40]. Scavenging of ROS by thyroid cancer cells in response to cytotoxic stimuli could at least in part be assigned to elevated redox protection. However, this protection of the cells against oxidative stress did not compromise the effectiveness of the drug.

2.3. Conclusion

In this work, neutral and cationic iridium(III) complexes of the type $[Ir(\eta^5\text{-}C_5Me_5)Cl_2\{Ph_2PCH_2S(O)_xPh\text{-}\kappa P\}]$ ($x = 0$, **1**; 1, **2**; 2, **3**) and $[Ir(\eta^5\text{-}C_5Me_5)Cl\{Ph_2PCH_2SPh\text{-}\kappa P,\kappa S\}][PF_6]$ (**4**), with bound diphenylphosphino-functionalized methyl phenyl sulfide, sulfoxide and sulfone ligands, were synthesized and fully characterized. Their biological potential was tested and proven against several cell lines. The following conclusions can be drawn:

1) *In vitro* tests revealed that the cytotoxic potency of the sulfur-functionalized phosphanes $Ph_2PCH_2S(O)_xPh$ is strongly increased by coordination to the $Ir(\eta^5\text{-}C_5Me_5)Cl_x$ (x = 1, 2) moiety. Thus, the cytotoxic activities were found up to forty times higher than those of the corresponding ligands, *cf.* the values given in Table 2 with those in Table S1.
2) The oxidation state of the sulfur (−SPh *vs.* −S(O)Ph *vs.* $-S(O)_2Ph$) in the ligands is directly correlated to the cytotoxic activity. Thus, complex **2** with the pendent sulfinyl exhibited the highest biological potential, followed by complexes **1** and **3** with the pendent sulfide and sulfonyl group, respectively, as demonstrated in Fig. 5.
3) In the case of the Ph_2PCH_2SPh ligand (**L1**) the coordination mode (κ*P vs.* κ*P*,κ*S*), which goes along with a transition from a neutral to a cationic complex (**1** *vs.* **4**), has no significant influence on the cytotoxic activity of the iridium(III) complexes (*cf.* Fig. 5).
4) The iridium(III) complex **2** with a sulfinyl functionalized-ligand possesses the highest potential to decrease the cell viability with an IC_{50} value of 1.9 μM against the A253 cell line.
5) The iridium(III) complexes **1**, **3**, and **4** with a sulfide- and sulfonyl-functionalized ligand showed comparable or even less cytotoxic activity in comparison with the related ruthenium(II) complexes $[Ru(\eta^6\text{-}p\text{-cym})Cl_2\{Ph_2PCH_2S(O)_xPh\text{-}\kappa P\}]/[Ru(\eta^6\text{-}p\text{-cym})Cl\{Ph_2PCH_2SPh\text{-}\kappa P,\kappa S\}][PF_6]$ (x = 0, 2; see Fig. 5 and the values given in Table 2 and Supplementary material S1). In contrast, the iridium(III) complex **2** with the sulfinyl-functionalized ligand was found up to ten times more active than the corresponding ruthenium(II) complex.

Table 2
IC_{50} values[a] (μM) of iridium(III) complexes **1**–**4** in comparison with cisplatin.

Compound	x[b]	518A2	8505C	A253	MCF-7	SW480
1	0 (κ*P*)	13.6 ± 2.3	15.4 ± 1.4	10.6 ± 1.3	18.5 ± 3.2	13.4 ± 3.0
2	1 (κ*P*)	2.4 ± 0.1	3.5 ± 0.5	1.9 ± 0.2	3.2 ± 0.4	2.3 ± 0.2
3	2 (κ*P*)	18.1 ± 1.6	36.8 ± 5.7	34.6 ± 1.1	42.0 ± 7.3	28.5 ± 11.7
4	0 (κ*P*,κ*S*)	9.8 ± 0.5	16.8 ± 3.5	10.2 ± 2.8	16.0 ± 1.9	14.6 ± 3.4
Cisplatin		1.5 ± 0.2	5.0 ± 0.2	0.8 ± 0.1	2.0 ± 0.1	3.2 ± 0.2

[a] Mean values ± SD (standard deviation) from three experiments.
[b] The coordination mode of the ligand is given in parentheses.

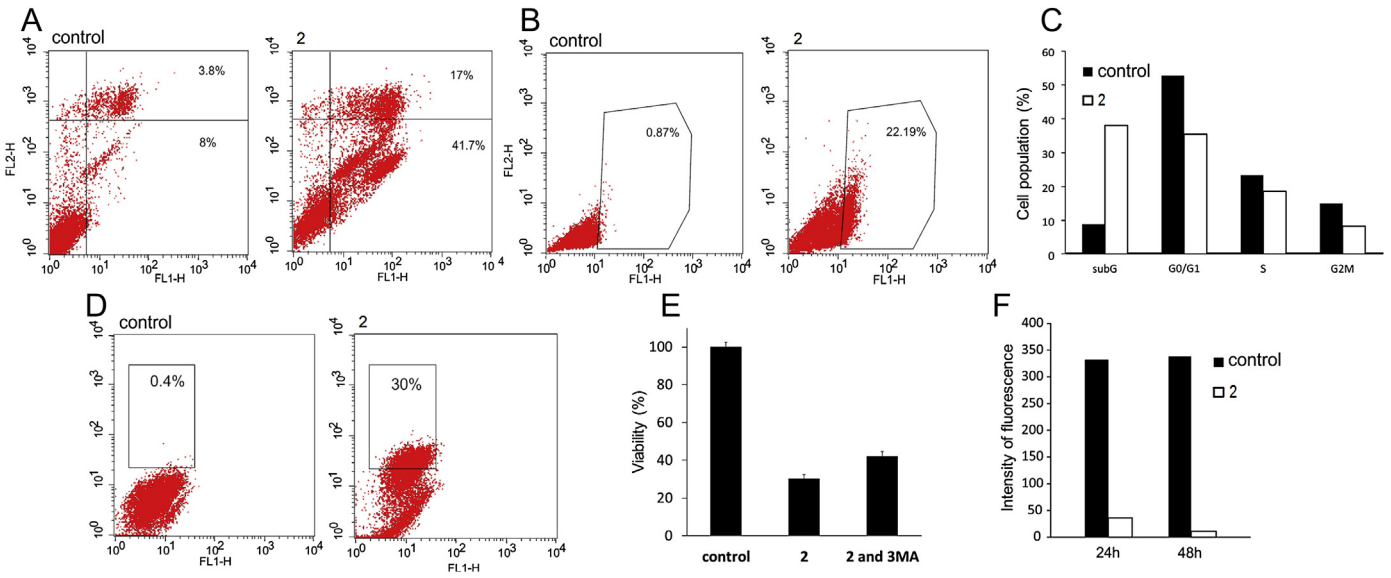

Fig. 4. The effect of [Ir(η^5-C_5Me_5)Cl_2{$Ph_2PCH_2S(O)Ph$-κ*P*}] (**2**) on malignant cell death. 8505C cells were exposed to IC_{50} doses of compound **2** and (A) apoptosis, (B) caspase activation, (C) cell cycle distribution, (D) presence of autophagic vesicles, (E) cell viability in presence of autophagic inhibitor (3-MA) or (F) production of ROS and RNS were evaluated.

In conclusion, in iridium(III) complexes of the type [Ir(η^5-C_5Me_5)Cl_2{$Ph_2PCH_2S(O)_x$Ph-κ*P*}] ($x = 0$–2; **1**–**3**) a correlation of the oxidation state of the sulfur atom at the pendent group to a decrease of the cell viability was observed, whereas complex **2** ($x = 1$) proved to be the most active against the 8505C and SW480 cell lines which display a low sensitivity to cisplatin. Additional experiments on cell line 8505C confirmed that apoptosis and autophagic cell death contribute to drug's tumoricidal action and that **2** significantly decreased the level of free radicals.

3. Experimental

3.1. General comments

All reactions and manipulations were carried out under argon using standard Schlenk techniques. Solvents were dried (*n*-pentane over Na/benzophenone; methanol over magnesium; methylene chloride over CaH_2) and freshly distilled prior to use. NMR spectra (^1H, ^{13}C, ^{31}P) were recorded at 27 °C on Varian Gemini 200 and VXR 400 spectrometers. Chemical shifts are relative to solvent signals (CD_2Cl_2, δ_H 5.32, δ_C 53.8) as internal references; δ_P is relative to external H_3PO_4 (85%). Microanalyses (C, H) were performed in the Microanalytical Laboratory of the University of Halle using a CHNS-932 (LECO) elemental analyzer. High-resolution ESI mass spectra were obtained from a Bruker Apex III Fourier transform ion cyclotron resonance (FTR-ICR) mass spectrometer (Bruker Daltonics) equipped with an Infinity cell, a 7.0 T superconducting magnet (Bruker), an rf-only hexapole ion guide, and an external APOLLO electrospray ion source (Agilent, off-axis spray). The sample solutions were introduced continuously via a syringe pump with a flow rate of 120 μL · h^{-1}. [{$IrCl_2(\eta^5$-$C_5Me_5)$}$_2$] and the ligands were prepared according to literature procedures [41,42].

3.2. Preparation of [$IrCl_2(\eta^5$-$C_5Me_5)${$Ph_2PCH_2S(O)_x$Ph-κ*P*}] (**1**–**3**)

The respective ligand (0.32 mmol) was added, with stirring to a methylene chloride solution (25 mL) of [{$IrCl_2(\eta^5$-$C_5Me_5)$}$_2$] (127 mg, 0.16 mmol). The solution was stirred at r.t. overnight yielding an orange powder which was filtered off, washed with *n*-pentane (3 × 2 mL), and dried under vacuum.

1 ($x = 0$). Yield: 153 mg (68%). HRMS (ESI): *m*/*z* Calc. for $[C_{29}H_{32}ClIrPS]^+$: 669.1251; found for $[M - Cl]^+$: 669.1243. Anal. Found: C, 49.01; H, 4.23. Calcd for $C_{29}H_{32}Cl_2IrPS$ (706.73): C, 49.29; H, 4.56. ^1H NMR (400 MHz, CD_2Cl_2): δ 1.26 (d, $^4J_{P,H} = 2.31$ Hz, 15H, CH_3), 4.29 (d, 2H, $^2J_{P,H} = 4.75$ Hz, CH_2), 6.85–7.87 (m, 15H, H_{Ph}). ^{13}C NMR (100 MHz, CD_2Cl_2): δ 8.2 (d, $^3J_{P,C} = 1.0$ Hz, CCH_3), 29.1 (d, $^1J_{P,C} = 26.8$ Hz, CH_2PPh_2), 92.2 (d, $^2J_{P,C} = 2.8$ Hz, CCH_3), 123.8–135.3 (C_{Ph}). ^{31}P NMR (162 MHz, CD_2Cl_2): δ 2.3 (s).

2 ($x = 1$). Yield: 164 mg (71%). HRMS (ESI): *m*/*z* Calc. for $[C_{29}H_{32}ClIrOPS]^+$: 685.1200; found for $[M - Cl]^+$: 685.1193. Anal. Found: C, 47.89; H, 4.17. Calcd for $C_{29}H_{32}Cl_2IrOPS$ (722.73): C, 48.19; H, 4.46. ^1H NMR (400 MHz, CD_2Cl_2): δ 1,37 (d, $^4J_{P,H} = 2.41$ Hz, 15H, CH_3), 4.04–4.57 (m, 2H, CH_2), 7.54–8.09 (m, 15H, H_{Ph}). ^{13}C NMR (100 MHz, CD_2Cl_2): δ 8.0 (d, $^3J_{P,C} = 1.0$ Hz, CCH_3), 55.9 (d, $^1J_{P,C} = 25.4$ Hz, CH_2PPh_2), 92.5 (d, $^2J_{P,C} = 3.0$ Hz, CCH_3), 123.8–135.3 (C_{Ph}). ^{31}P NMR (162 MHz, CD_2Cl_2): δ −4.8 (s).

3 ($x = 2$). Yield: 151 mg (64%). HRMS (ESI): *m*/*z* Calc. for $[C_{29}H_{32}ClIrO_2PS]^+$: 701.1149; found for $[M - Cl]^+$: 701.1140. Anal. Found: C, 47.34; H, 4.51. Calcd for $C_{29}H_{32}Cl_2IrO_2PS$ (738.72): C, 47.15; H, 4.37. ^1H NMR (400 MHz, CD_2Cl_2): δ 1.33 (d, $^4J_{P,H} = 2.39$ Hz, 15H, CH_3), 3.96–4.01 (d, 1H, CH_2), 4.61–4.66 (d, 1H, CH_2), 7.31–8.08 (m, 15H, H_{Ph}). ^{13}C NMR (100 MHz, CD_2Cl_2): δ 8.3 (s, CCH_3), 56.5 (d, $^1J_{P,C} = 26.0$ Hz, CH_2PPh_2), 92.5 (s, CCH_3), 124.0–135.5 (C_{Ph}). ^{31}P NMR (162 MHz, CD_2Cl_2): δ −5.2 (s).

3.3. Preparation of [$IrCl(\eta^5$-$C_5Me_5)${Ph_2PCH_2SPh-κ*P*,κ*S*}][PF_6] (**4**)

The respective ligand (0.32 mmol) was added, with stirring, to a methanol solution (30 mL) of [{$IrCl_2(\eta^5$-$C_5Me_5)$}$_2$] (127 mg, 0.16 mmol) and the solution was heated under reflux for 3 h. Subsequently, [NH_4][PF_6] (6 equiv.) was added. After storage at −70 °C overnight, the precipitate obtained was filtered off, washed with diethyl ether (3 × 2 mL), and dried under vacuum. Yield: 201 mg (77%).

HRMS (ESI): *m*/*z* Calc. for $[C_{29}H_{32}ClIrPS]^+$: 669.1251; found for $[M]^+$: 669.1258. Anal. Found: C, 42.93; H, 4.12. Calcd for $C_{29}H_{32}ClF_6IrP_2S$ (816.24): C, 42.67; H, 3.95. ^1H NMR (400 MHz,

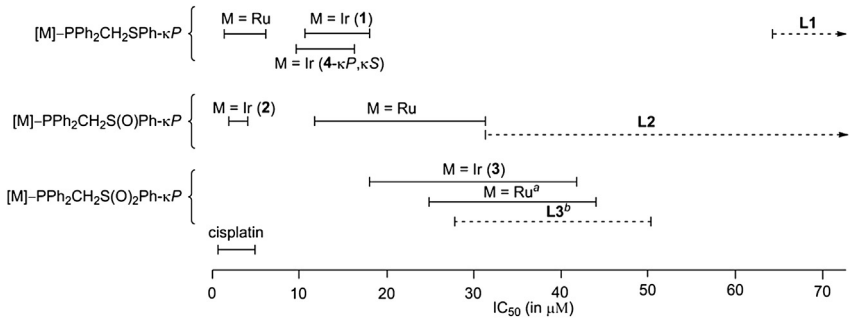

Fig. 5. Range of the cytotoxic activity (based on the IC_{50} values for the five cell lines under investigation) of the iridium(III) complexes **1**–**4** ([Ir] = Ir(η^5-C_5Me_5)Cl_x; x = 1, 2) and of the related ruthenium(II) complexes [Ru(η^6-*p*-cym)Cl_2{$Ph_2PCH_2S(O)_x$Ph-κ*P*}] ([Ru] = Ru(η^6-*p*-cym)Cl_2). For comparison, the corresponding values of cisplatin and the uncoordinated ligands $Ph_2PCH_2S(O)_x$Ph **L1**–**L3** (dashed lines) are given. [a]Four values; exception cell line MCF-7 (IC_{50} = 115.0 μM). [b]Four values; exception cell line 518A2 (IC_{50} = 5.5 μM).

CD_2Cl_2): δ 1.73 (d, $^4J_{P,H}$ = 2.91 Hz, 15H, CH_3), 5.12–5.18 (m, 1H, CH_2), 7.20–7.25 (m, 1H, CH_2), 7.20–7.71 (m, 15H, H_{Ph}). ^{13}C NMR (100 MHz, CD_2Cl_2): δ 8.7 (d, $^3J_{P,C}$ = 1.0 Hz, CCH_3), 29.6 (s, CH_2PPh_2), 92.3 (s, CCH_3), 123.8–133.7 (C_{Ph}). ^{31}P NMR (162 MHz, CD_2Cl_2): δ −31.9 (s), −143.9 (sept, $^1J_{P,F}$ = 709.0 Hz, PF_6).

3.4. X-ray crystallography

Data for X-ray diffraction analyses of single crystals of **2** were collected on an Oxford Gemini S diffractometer at 293 K using Cu-*Kα* radiation (λ = 1.54184 Å, graphite monochromator). A summary of the crystallographic data, the data collection parameters, and the refinement parameters are given in Table 3. Multiscan corrections were applied using the SCALE3 ABSPACK (T_{min}/T_{max}: 0.45/1.00) [43,44]. The structure was solved with direct methods using SHELXS-97 and refined using full-matrix least-square routines against F^2 with SHELXL-97 [45,46]. All non-hydrogen atoms were refined with anisotropic displacement parameters and hydrogen atoms with isotropic ones. H atoms were placed in calculated positions according to the riding model. The $PhS(O)CH_2$ group was found to be disordered over two positions with occupancies of 63% and 37%. Furthermore, some restraints had to be used for the refinement of the sulfinyl group, methyl group, and the phenyl ring (DELU, SIMU, ISOR). CCDC 936713 contains the supplementary crystallographic data for this paper. These data can be obtained free of charge from the Cambridge Crystallographic Data Centre via www.ccdc.cam.ac.uk/data_request/cif.

Table 3
Crystallographic data, data collection parameters, and refinement parameters for **2**.

	2
Empirical formula	$C_{29}H_{32}Cl_2IrOPS$
M_r	722.68
Crystal System	Orthorhombic
Space group	$P2_12_12_1$
a/Å	8.5463(7)
b/Å	17.9984(13)
c/Å	18.2025(14)
V/Å^3	2799.9(4)
Z	4
D_{cal}/g cm^{-3}	1.714
μ(Cu-Kα)/mm^{-1}	12.381
F(000)	1424
θ range/°	3.4438–65.8701
Rfln collected	5488
Refln observed [$I > 2\sigma(I)$]	3568
Rfln independent	3829 (R_{int} = 0.0395)
Data/restraints/parameters	3829/397/358
Goodness-of-fit on F^2	1.040
$R1$, $wR2$ [$I > 2\sigma(I)$]	0.0564, 0.1437
$R1$, $wR2$ (all data)	0.0601, 0.1464
Largest diff. peak and hole/e Å^{-3}	1.870/−1.191

3.5. In vitro antitumoral studies

3.5.1. Reagents and cells

Fetal calf serum (FCS), RPMI-1640, phosphate-buffered saline (PBS), dimethyl sulfoxide (DMSO), and propidium iodide (PI) were obtained from Sigma (St. Louis, MO). Annexin V-FITC (AnnV) was from Biotium (Hayward, CA). Acridin orange (AO) was from Labo-Moderna (Paris, France). Apostat was purchased from R&D (R&D Systems, Minneapolis, MN USA). Human thyroid carcinoma 8505C, submandibular gland carcinoma A253, breast adenocarcinoma MCF7, melanoma 518A2 and colon cancer SW480 were obtained from ATCC. Cells were routinely maintained in HEPES-buffered RPMI-1640 medium supplemented with 10% FCS, 2 mM L-glutamine, 0.01% sodium pyruvate, 5×10^{-5} M 2-mercaptoethanol, and antibiotics (culture medium) at 37 °C in a humidified atmosphere with 5% CO_2. After standard trypsinization, cells were seeded at 1×10^4–2.5×10^3/well in 96-well plates for viability determination and 1.5×10^5/well in 6-well plate for flow cytometry. Stock solutions of investigated compounds were prepared in dimethyl sulfoxide (DMSO, Sigma Aldrich) at a concentration of 20 mM, filtered through Millipore filter, 0.22 μm, before use, and diluted by nutrient medium to various working concentrations. Final concentrations achieved in treated wells were 0.78, 1.56, 3.12, 6.25, 12.5, 25.0 and 50.0 μM.

3.5.2. Determination of cell viability by sulphorhodamine assay (SRB)

The viability of adherent viable cells was measured by SRB assay [38]. Cells were exposed to a wide range of doses of the drugs for 96 h and then fixed with 10% of TCA for 2 h at 4 °C. After fixation, cells were washed in distilled water, stained with 0.4% SRB solution 30 min at RT, washed and dried overnight. The dye was dissolved in 10 mM TRIS Buffer and the absorbance was measured at 540 nm with the reference wavelength at 640 nm. Results are expressed as percentage of control that was arbitrarily set to 100%.

3.5.3. Cell cycle analysis

Cells were treated with IC_{50} dose of [Ir(η^5-C_5Me_5)Cl_2{$Ph_2PCH_2S(O)$Ph-κ*P*}] (**2**) for 48 h, trypsinized, and fixed in 70% ethanol at 4 °C over-night. Cells were thoroughly washed in PBS, and stained with solution containing PI (20 μg/ml) and RNase (0.1 mg/ml) for 30 min at 37 °C in dark. Red fluorescence was analyzed with FACSCalibur flow cytometer (BD, Heildelberg, Germany). The distribution of cells in different cell cycle phases was determined with Cell Quest Pro software (BD) [47].

3.5.4. AnnexinV-FITC/PI, AO staining and caspase detection

Cells were exposed to IC_{50} dose of [Ir(η^5-C_5Me_5)Cl_2{$Ph_2PCH_2S(O)Ph$-κ*P*}] (**2**) for 48 h. After trypsinization, cells were stained with AnnV-FITC/PI (Biotium, Hayward, CA) or Apostat according to the manufacturer's instructions. Alternatively, cells were stained with a solution of 100 mM AO for 15 min at 37 °C. Cells were analyzed with FACSCalibur flow cytometer (BD, Heidelberg, Germany) using Cell Quest Pro software (BD).

3.5.5. Measurement of ROS generation

The production of reactive oxygen and nitrogen species was determined by redox-sensitive dye, dihydrorhodamine 123 (DHR). The cells were stained with 1 μM DHR for 20 min before treatment with [Ir(η^5-C_5Me_5)Cl_2{$Ph_2PCH_2S(O)Ph$-κ*P*}] (**2**). After 24 or 48 h incubation, the cells were detached, washed in PBS, and the fluorescence intensity was analyzed with a FACSCalibur flow cytometer using Cell Quest Pro software.

Results are presented as mean ± standard deviation (SD) of triplicate observations from the representative of three experiments, unless indicated otherwise. The significance of the difference between treatments and control was analyzed by ANOVA followed by the Student–Newman–Keuls, test $P < 0.05$ was considered significant.

Acknowledgments

G. L. gratefully acknowledges financial support from Graduiertenförderung des Landes Sachsen-Anhalt. The authors (University of Belgrade) would like to acknowledge financial support from the Ministry of Science and Technological Development of the Republic of Serbia (Grant No. 173013) and Dr. Jürgen Schmidt (Department of Bioorganic Chemistry, Leibniz Institute of Plant Biochemistry) for the high-resolution ESI mass spectra.

Appendix A. Supplementary data

Supplementary data related to this article can be found at http://dx.doi.org/10.1016/j.ejmech.2013.08.025.

References

[1] G. Jaouen, Bioorganometallics, first ed., Wiley-VCH, Weinheim, 2005.
[2] B. Rosenberg, L. van Camp, T. Krigas, Nature 205 (1965) 698–699.
[3] B. Rosenberg, L. van Camp, J.E. Trosko, V.H. Mansour, Nature 222 (1969) 385–386.
[4] B. Lippert, Cisplatin: Chemistry and Biochemistry of a Leading Anticancer Drug, first ed., Wiley-VCH, Weinheim, 1999.
[5] G. Chu, J. Biol. Chem. 269 (1994) 787–790.
[6] E. Wong, C.M. Giandomenico, Chem. Rev. 99 (1999) 2451–2466.
[7] M. Galanski, M.A. Jakupec, B.K. Keppler, Curr. Med. Chem. 12 (2005) 2075–2094.
[8] S.H. v. Rijt, P.J. Sadler, Drug Discovery Today 14 (2009) 1089–1097.
[9] M.J. Clarke, F. Zhu, D.R. Frasca, Chem. Rev. 99 (1999) 2511–2534.
[10] Z. Guo, P.J. Sadler, Angew. Chem. Int. Ed. 38 (1999) 1512–1531.
[11] J.C. Dabrowiak, Metals in Medicine, first ed., Wiley-VCH, Weinheim, 2009.
[12] M. Cocchietto, G. Sava, Pharmacol. Toxicol. 87 (2000) 193–197.
[13] G. Sava, A. Bergamo, Int. J. Oncol. 17 (2000) 353–365.
[14] R. Gagliardi, G. Sava, S. Pacor, G. Mestroni, E. Alessio, Clin. Exp. Metastasis 12 (1994) 93–100.
[15] C.G. Hartinger, S. Zorbas-Seifried, M.A. Jakupec, B. Kynast, H. Zorbas, B.K. Keppler, J. Inorg. Biochem. 100 (2006) 891–904.
[16] J.M. Rademaker-Lakhai, D. van den Bongard, D. Pluim, J.H. Beijnen, J.H.M. Schellens, Clin. Cancer Res. 10 (2004) 3717–3727.
[17] M.A. Jakupec, V.B. Arion, S. Kapitza, E. Reisner, A. Eichinger, M. Pongratz, B. Marian, N.Graf v. Keyserlingk, B.K. Keppler, Int. J. Clin. Pharmacol. Ther. 43 (2005) 595–596.
[18] S.J. Lucas, R.M. Lord, R.L. Wilson, R.M. Phillips, V. Sridharan, P.C. McGowan, Dalton Trans. 41 (2012) 13800–13802.
[19] K.K.W. Lo, K.Y. Zhang, RSC Adv. 2 (2012) 12069–12083.
[20] Y. Geldmacher, M. Oleszak, W.S. Sheldrick, Inorg. Chim. Acta 393 (2012) 84–102.
[21] H. Amouri, J. Moussa, A.K. Renfrew, P.J. Dyson, M.N. Rager, L.-M. Chamoreau, Angew. Chem. Int. Ed. 49 (2010) 7530–7533.
[22] S. Wirth, C.J. Rohbogner, M. Cieslak, J. Kazmierczak-Baranska, S. Donevski, B. Nawrot, I.-P. Lorenz, J. Biol. Inorg. Chem. 15 (2010) 429–440.
[23] A. Casini, F. Edafe, M. Erlandsson, L. Gonsalvi, A. Ciancetta, N. Re, A. Ienco, L. Messori, M. Peruzzini, P.J. Dyson, Dalton Trans. 39 (2010) 5556–5563.
[24] M. Gras, B. Therrien, G. Süss-Fink, A. Casini, F. Edafe, P.J. Dyson, J. Organomet. Chem. 695 (2010) 1119–1125.
[25] C.G. Hartinger, Angew. Chem. Int. Ed. 49 (2010) 8304–8305.
[26] L. Helm, A.E. Merbach, Coord. Chem. Rev. 187 (1999) 151–181.
[27] G. Marcon, A. Casini, P. Mura, L. Messori, A. Bergamo, P. Orioli, Met.-Based Drugs 7 (2000) 195–200.
[28] Y. Geldmacher, I. Kitanovic, H. Alborzinia, K. Bergerhoff, R. Rubbiani, P. Wefelmeier, A. Prokop, R. Gust, I. Ott, S. Wölfl, W.S. Sheldrick, Chem. Med. Chem. 6 (2011) 429.
[29] Z. Liu, A. Habtemariam, A.M. Pizarro, S.A. Fletcher, A. Kisova, O. Vrana, L. Salassa, P.C.A. Bruijnincx, G.J. Clarkson, V. Brabec, P.J. Sadler, J. Med. Chem. 54 (2011) 3011–3026.
[30] S. Schäfer, I. Ott, R. Gust, W.S. Sheldrick, Eur. J. Inorg. Chem. (2007) 3034–3046.
[31] Z. Liu, L. Salassa, A. Habtemariam, A.M. Pizarro, G.J. Clarkson, P.J. Sadler, Inorg. Chem. 50 (2011) 5777–5783.
[32] Z. Liu, A. Habtemariam, A.M. Pizarro, G.J. Clarkson, P.J. Sadler, Organometallics 30 (2011) 4702–4710.
[33] G. Ludwig, G.N. Kaluđerović, M. Bette, M. Block, R. Paschke, D. Steinborn, J. Inorg. Biochem. 113 (2012) 77–82.
[34] G. Ludwig, G.N. Kaluđerović, T. Rüffer, M. Bette, M. Korb, M. Block, R. Paschke, H. Lang, D. Steinborn, Dalton Trans. 42 (2013) 3771–3774.
[35] M. Valderrama, R. Contreras, D. Boys, Polyhedron 16 (1997) 1811–1817.
[36] M. Erlandsson, V.R. Landaeta, L. Gonsalvi, M. Peruzzini, A.D. Phillips, P.J. Dyson, G. Laurenczy, Eur. J. Inorg. Chem. (2008) 620–627.
[37] Cambridge Structural Database (ConQuest), Version 1.15, Crystallographic Data Centre, University Chemical Laboratory, Cambridge, UK, 2013.
[38] P. Skehan, R. Storeng, D. Scudiero, A. Monks, J. McMahon, D. Vistica, J.T. Warren, H. Bokesch, S. Kenney, M.R. Boyd, J. Natl. Cancer Inst. 82 (1990) 1107–1112.
[39] Z.-X. Du, H.-Y. Zhang, X. Meng, Y. Guan, H.-Q. Wang, BMC Cancer 9 (2009) 56.
[40] Z.-X. Du, Y. Yan, H.-Y. Zhang, B.-Q. Liu, Y.-Y. Gao, X.-F. Niu, X. Meng, H.-Q. Wang, J. Clin. Endocrinol. Metab. 96 (2011) E763–E771.
[41] R.G. Ball, W.A.G. Graham, D.M. Heinekey, J.K. Hoyano, A.D. McMaster, B.M. Mattson, S.T. Michel, Inorg. Chem. 29 (1990) 2023–2025.
[42] M. Block, M. Bette, C. Wagner, D. Steinborn, Z. Anorg. Allg. Chem. 637 (2011) 206–210.
[43] (a) MULscanABS, PLATON for Windows Taskbar v1.15, University of Glasgow, 2008;
(b) A.L. Spek, J. Appl. Crystallogr. 36 (2003) 7.
[44] SCALE3 ABSPACK, Empirical Absorption Correction, CrysAlis–Software package, Oxford Diffraction Ltd, 2006.
[45] G.M. Sheldrick, SHELXS-97, Program for Crystal Structure Solution, University of Göttingen, Göttingen, 1998.
[46] G.M. Sheldrick, SHELXL-97, Program for the Refinement of Crystal Structures, University of Göttingen, Göttingen, 1997.
[47] G.N. Kaluđerović, S. Mijatović, B.B. Zmejkovski, M.Z. Bulatović, S. Gomez-Ruiz, M. Mojić, D. Steinborn, D. Miljković, H. Schmidt, S.D. Stošić-Grujičić, T.J. Sabo, D. Maksimović-Ivanić, Metallomics 4 (2012) 979–987.